Vol 14 No 5, May 2005
1009-1963/2005/14(05)/1051-04

Chinese Physics

© 2005 Chin. Phys. Soc.
and IOP Publishing Ltd

Preisach analysis of $(La_{0.2}Nd_{0.8})_{0.67}Pb_{0.33}MnO_3$

Cao Xian-Sheng(曹先胜)[a)†], Xiao Chun-Tao(肖春涛)[b)],
Gywn Williams[c)], and Roy Roshko[c)]

[a)] *Material Department, The Second Northwest University for Nationalities, Ningxia 750021, China*
[b)] *Physics Department, Lanzhou University, Lanzhou 730000, China*
[c)] *Department of Physics and Astronomy, University of Manitoba, R3T 2N2, Canada*

(Received 25 November 2004; revised manuscript received 21 December 2004)

The perovskite $(La_{0.2}Nd_{0.8})_{0.67}Pb_{0.33}MnO_3$ (LNPMO) with a Curie temperature T_C=220K is characterized by measuring the zero field cooled (ZFC) and field cooled (FC) moments over a wide range of temperature 2K< T <290K in an applied field of H_a=3978.87A/m, and also by the major hysteresis loop over the field range $|H_a|\leq$1061kA/m at T=10K. The data analysed within the framework of a generalized Preisach model, which includes thermal fluctuations, critical effects, and a temperature-dependent distribution of free energy barriers. The analysis shows that the response function of LNPMO is dominated by the growth of the anisotropy barriers.

Keywords: Preisach model, hysteresis loop, magnetization
PACC: 7540M, 7530C, 7460E, 7500

1. Introduction

Substituted perovskite systems $Re_{1-x}Pb_xMnO_3$ are currently of considerable interest from both fundamental research and technological application.[1−4] The characterization of irreversible behaviour in these materials, which is typically based on certain standard experimental protocols such as the major hysteresis loop, or the temperature dependence of the moment measured under zero field cooled (ZFC) and field cooled (FC) conditions, tends to suffer from the lack of a formal theoretical framework for the interpretation of such common structural features as the peak in the ZFC moment, or the degree of bifurcation of the FC and ZFC branches. In this article, we describe a recent model for irreversibility in magnetically ordered materials which provides such a framework, and we apply this model to the analysis of hysteresis data and FC/ZFC data in a doped perovskite $(La_{0.2}Nd_{0.8})_{0.67}Pb_{0.33}MnO_3$ (LNPMO). It is shown that the model is able to replicate the characteristics of the experimental data in remarkable detail and allows us to define the extent to which intrinsic anisotropy effects and thermal fluctuation effects, which both contribute to shaping the temperature dependence of the macroscopic response of the LNPMO.

2. Experiment

Samples with nominal compositions LNPMO were prepared by conventional ceramic techniques. Stoichiometric quantities of ultrapure (La_2O_3, Nd_2O_3, PbO, MnO_2) were mixed for 24h by ball milling in acetone, pressed into pellet form, heated in air at 850°C for 24h, hand ground with a binder, granulated, pressed into a disc shape, and sintered for 72h in air at 1100°C for obtaining the manganese perovskite. Magnetic measurements were performed as a function of both applied field and temperature in a Quantum Design MPMS model 6000 system. X-ray diffraction data acquired using a Philips PW1710 automated diffraction system with a Bragg–Brentano goniometer confirm a single-phased rhombohedral structure. The lattice parameters of the LNPMO are α=0.77719(±0.00008)nm, and θ= 90.19 (±0.01)°.

3. Analysis

Figure 1 shows the temperature dependence of the FC and ZFC moments measured in a low applied field H_a=3978.87A/m, and Fig.2 shows the major hysteresis loop measured at T=10K, for the doped lanthanum perovskite LNPMO. For this material, the FC and ZFC data were measured on warming in the field H_a, after first cooling the system to T=10K in the

†E-mail: cxsheng@eyou.com

field H_a and in zero field, respectively, from a temperature in the paramagnetic regime above T_C. The discrete points in these figures are experimental data and the solid curves are numerical Preisach simulations. The solid curves in Figs.1–3 are numerical simulations based on the extended Preisach model described earlier, and the corresponding fitting parameters for the LNPMO are listed in Table 1.

Table 1. Preisach fitting parameters.

T_C/K	H_{c0}/(A/m)	σ_{c0}	σ_{i0}/(A/m)		μ_0/(A·m^2)	Γ
220	10160	8.5	11544.6		6.8×10^{-16}	0.32
Γ_c	Γ_c'	Γ_i	λ/(m/A)	f	m_{sat}/(A·m^2)	$\ln(t_{exp}/\tau_0)$
3.19	5.6	0.5	7.28×10^{-6}	0.30	4.7×10^{-3}	25

A comparison between the two curves in Fig.1 reveals a number of structural similarities in the temperature dependence of the FC and ZFC moments for the LNPMO. In this system, the data are characterized by a bifurcation temperature which roughly coincides with the critical ordering temperature, T_C=220K for the manganese perovskite. Above the bifurcation temperature, the FC and ZFC moments are essentially identical and the material behaves like paramagnetic compound, while below the bifurcation temperature the two branches diverge very strongly, indicating the start of irreversible behaviour. The FC moment varies monotonically with temperature, while the ZFC moment exhibits a peak close to T_C. The mayor hysteresis loops in Fig.2 show that the manganese perovskite with $H_c(T=10\text{K})\approx8.76$kA/m.

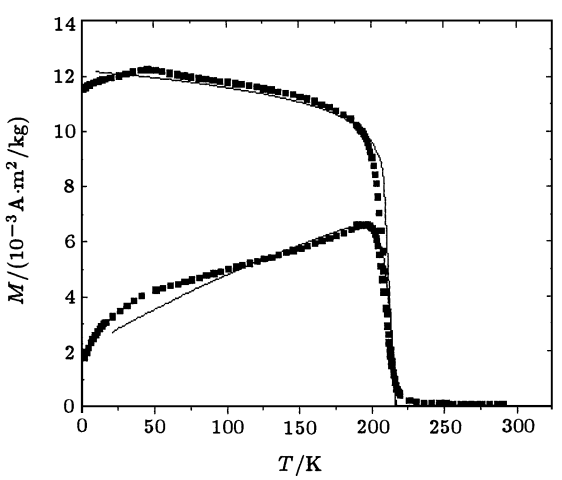


Fig.1. Temperature dependence of the FC and ZFC moment of LNPMO measured in an applied field H_a=3978.87A/m. The discrete points are experimental data and the solid curves are numerical simulations.

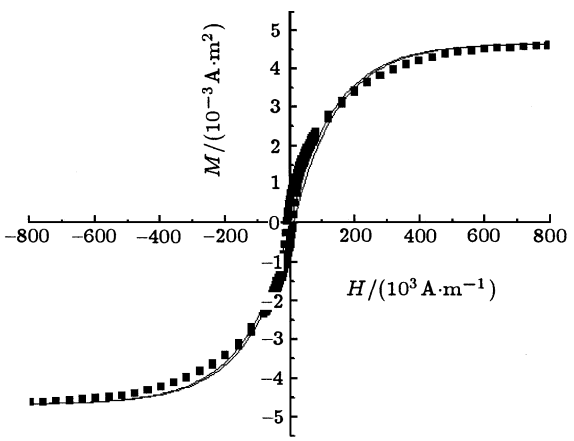


Fig.2. Major hysteresis loop for LNPMO measured at T=10K. The discrete points are experimental data and the solid curve is numerical simulation.

The data have been analysed within the framework of a generalized Preisach model of hysteresis.[5–7] The essential elements of the model are as follows. It is assumed that all magnetic systems can be regarded as an ensemble of bistable subsystems, each with a moment M, two states $\varphi = \pm M$, and two free energy barriers $W_\pm$, which can be represented by two equivalent fields: a coercive field $H_c=(W_+ + W_-)/2M$ and an interaction field $H_i=(W_+ - W_-)/2M$. A specific magnetic material is characterized by a distribution of these fields:

$$p(H_i, H_c, T) = \delta(M, M_0(T))(2\pi\sigma_c^2 H_c^2)^{-1/2}\exp \times(-\log[H_c/H_c(T)]^2/2\sigma_c^2)(2\pi\sigma_i^2)^{-1/2} \times \exp(-H_i^2/2\sigma_i^2).$$

The application of an external field[8] distorts the free energy barriers to $W'_{\pm} = W_{\pm} \pm MH_a$, and induces transitions whenever $W'_{\pm}$=0. Temperature enters the model in two ways. One of these is thermal fluctuations, which effectively reduce all of the free energy barriers $W'_{\pm}$ by $W^*(T) = k_B T \ln(t_{exp}/\tau_0)$, where $\tau_0(\cong 10^{-9}s)$ is a microscopic time and t_{exp} is the experimental time constant, and are described by an equivalent thermal viscosity field H^*_T=W^*/M. The other is variations in the intrinsic properties of the subsystems themselves with temperature, which include the critical behaviour of the spontaneous moment $M(T) = M_0(1 - T/T_C)^{\Gamma}$, as well as the related temperature-dependent growth of the free energy barriers $W_{\pm}(T)$, which are represented by introducing power law temperature dependence into the Preisach distribution parameters $H_c(T) = H_{c0}(1 - T/T_C)^{\Gamma_c}$, $\sigma_c = \sigma_{c0}(1 - T/T_C)^{\Gamma'_c}$, $\sigma_i = \sigma_{i0}(1 - T/T_C)^{\Gamma_i}$. The temperature dependence of the free energy is thus defined by the four exponents Γ, Γ_c, Γ_i and Γ'_c. The parameter Γ plays the same role as the critical exponent β employed in the critical analysis. Both field induced and thermally induced transitions are represented geometrically by instability lines in the Preisach plane (H_c, H_i), and these have been exploited to construct geometrical representations for the FC and ZFC protocols, as well as for magnetizing curves and hysteresis loop.

In this article, we focus particularly on the FC/ZFC response in the low field limit since this is where the influence of the critical behaviour arising from the collapse of the barrier distribution as $T \to T_C$ is most evident. In both cases, the fits show that the behaviours of the FC and ZFC branches are dominated by different physical mechanisms: the shape of the ZFC branch is determined primarily by thermal fluctuations H^*_T and by the collapse of the median coercive field $H_c(T)$, while the FC branch is sensitive to the temperature dependence of the spontaneous moment $M(T)$ and the interaction fields $\sigma_i(T)$. Thus, in the LNPMO, the gradual increase in the ZFC moment with temperature increasing originates from thermal overbarrier activation, as defined by H^*_T=$W^*(T)/m_0$, while the peak is a consequence of a competition between the variations of the coercive field $H_c(T)$=(10160A/m)$(1 - T/T_C)^{3.19}$ and the spontaneous moment $M(T)$=$(6.8\times10^{-16}A\cdot m^2)$ $(1 - T/T_C)^{0.32}$ with temperature. By contrast, the amplitude and the shape of the FC branch are defined by σ_{i0} and by the exponents Γ_i and Γ. The pronounced bifurcation of the ZFC and FC branches in the low applied fields is a consequence of two inequalities,[9] $\sigma_{i0} > H_a$, FC keeps constant below T_C, then decreases quickly to zero at T_C, and $H_a > \bar{H}_c$ which ensures that the ZFC has a peak near T_C. The fit to the hysteresis loop in Fig.2 is achieved by supplementing the Preisach response with a reversible component, so that $M = M_{sat}\{(1 - f)M_{Preisach} \pm f[1 - \exp(\lambda |H_a|)]\}$ with $0 \le f \le 1$, and the parameters f and λ are also included in Table 1. The model contains two characteristic energies, which allow us to quantify the relative effectiveness of thermal fluctuations and intrinsic effects. One of these is the mean zero temperature anisotropy barrier $\bar{W}_a(0) = M_0\bar{H}_{c0}$, and the other is the critical thermal fluctuation energy $W^*_c = k_B T_c \ln(t_{exp}/\tau_0)$. For the LNPMO, $\bar{W}_a(0) = \mu_0 H_{c0}$=$8.677\times10^{-18}$J, and $W^*_c \equiv k_B T_C \ln(t_{exp}/\tau_0)$=$7.59\times10^{-19}$J, so $\eta = \bar{W}_a(0)/W^*_c = 11.43$, showing that $\bar{W}_a(0) \gg W^*_c$. Thermal fluctuations are expected to play a relatively minor role in defining the temperature dependence of the magnetic response functions. So, the LNPMO is anisotropy-dominated.

Figure 3 shows a comparison between the temperature dependence of the mean anisotropy barrier obtained from the fits, normalized to $\bar{W}_a(0)$, $\bar{W}_a(T)/\bar{W}_a(0)$=$(1-T/T_C)^{\Gamma_C}$ $(1-T/T_C)^{\Gamma}$ and the normalized thermal fluctuation energy $W^*(T)/\bar{W}_a(0) = [k_B T/\bar{W}_a(0)] \ln(t_{exp}/\tau_0)$. The intersection of the two curves determines the mean blocking temperature $T_{blocking}$=205K, above which the system is superparamagnetic, and below which the system response is irreversible.

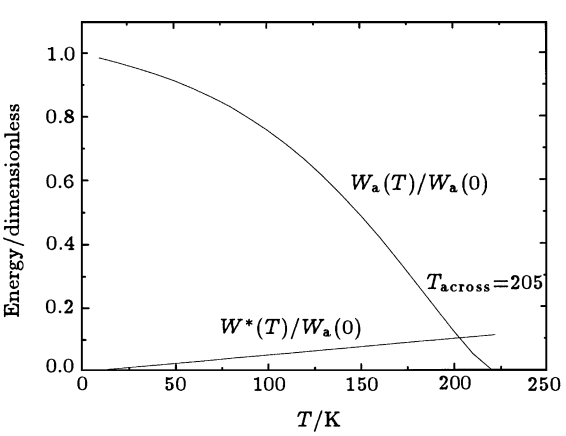


Fig.3. Temperature dependence of the mean anisotropy barrier $\bar{W}_a(T)/\bar{W}_a(0)$ in obtained from the numerical simulations, and the thermal fluctuation energy $W^*(T)/\bar{W}_a(0)$.

4. Conclusions

The data are analysed within the framework of a generalized version of the Preisach model, which combines thermal fluctuations with the growth of the free energy barriers. The numerical simulations match the major features of the ZFC/FC magnetization, and reproduce the details of the spectrum of Barhausen instabilities in this material. Such analyses provide compelling support for the validity of the Preisach model as a physical representation of irreversibility in practical magnetic systems.

References

[1] Jin S *et al* 1994 *Science* **264** 413
[2] Schiffer P, Raminez A P, Bao W and Cheong S W 1995 *Phys. Rev. Lett.* **75** 3336
[3] Zhang F X *et al* 1998 *Acta Phys. Sin.* **47** 112 (in Chinese)
[4] Zhong W *et al* 2003 *Chin. Phys. Lett.* **20** 742
[5] Zhao J H *et al* 2001 *J. Appl. Phys.* **89** 7248
[6] Preisach F 1935 *Z. Phys.* **94** 277
[7] Xiao Ch T and Cao X Sh 2004 *Acta Phys. Sin.* **53** 2347 (in Chinese)
[8] Liu W M, Zhang W S, Pu F C and Zhou X 1999 *Phys. Rev.* B **60** 12893
[9] Hou D L *et al* 2003 *J. Magn. Magn. Mater.* **253** 279